We are IntechOpen, the world's leading publisher of Open Access books Built by scientists, for scientists

4,800
Open access books available

122,000
International authors and editors

135M
Downloads

Our authors are among the

154
Countries delivered to

TOP 1%
most cited scientists

12.2%
Contributors from top 500 universities

CLARIVATE ANALYTICS BOOK CITATION INDEX INDEXED

WEB OF SCIENCE™

Selection of our books indexed in the Book Citation Index in Web of Science™ Core Collection (BKCI)

Interested in publishing with us?
Contact book.department@intechopen.com

Numbers displayed above are based on latest data collected.
For more information visit www.intechopen.com

Chapter 3

Solid-Liquid-Solid Interfaces

Jeffrey L. Streator

Additional information is available at the end of the chapter

http://dx.doi.org/10.5772/61572

Abstract

Interfaces comprised of a liquid interposed between two solids in close proximity are common in small-scale devices. In many cases, the liquid induces large and undesired adhesive forces. It is of interest, therefore, to model the way in which forces are developed in such an interface. The following chapter presents several models of liquid-mediated adhesion, considering the roles of surface geometry, liquid surface tension, elastic deformation, surface roughness, and surface motion on the development of interfacial forces.

Keywords: Capillary film, liquid-mediated adhesion, liquid bridge

1. Introduction

Phenomena related to the wetting of solid–solid interfaces are of technological importance. When two surfaces are in close proximity, the presence of a liquid film may cause the surfaces to stick together. Such liquid-mediated adhesion can negatively affect the operation of micro/nanoscale systems [1–7]. The interfacial liquid film, which may be present due to condensation, contamination, or lubrication, may experience large concave curvatures at the liquid-vapor interface and large negative pressures. These negative pressures give rise to large adhesive forces, which can have a potentially deleterious effect on the performance of small-scale devices.

In this chapter, we will discuss the behavior of an interface comprised of a liquid interposed between two solids. Throughout this chapter, we are concerned with the role of liquid films in regimes where gravitational effects are negligible, which generally implies that the vertical length scale is small. As an illustration, it can be easily shown that the change in pressure due to gravity within a near-hemispherical water droplet (resting on a horizontal surface) from just within the top of the free surface to the bottom of the droplet is given by $(\Delta p)_{gravity} = \rho g R$, where ρ is the water mass density, g is the gravitational acceleration, and R is the approximate radius

of the droplet. By comparison, the change in pressure across the free surface of the droplet is given by $(\Delta p)_{surface\ tension} = 2\gamma / R$, where γ is the liquid surface tension. Thus, the ratio of gravitational effects to surface tension effects is equal to $\rho g R^2 / 2\gamma$. For water at room temperature (and ambient pressure), one has ρ = 1000 kg/m^3 and γ = 0.0727 N/m, so that for a radius of 1.0 mm, we have a ratio of about 0.07, meaning that the change in pressure due to gravity is only about 7% of that due to surface tension. Moreover, it is seen that the relative effects of gravity decrease in proportion to the square of the droplet radius. In general, the smaller the vertical scale, the less important are the effects of gravity in comparison to those of surface tension.

Of particular interest in this chapter is the topic of liquid-mediation adhesion, a mechanism by which the liquid film pulls inward on the solid surfaces. We consider the effects of liquid surface tension, liquid viscosity, surface geometry, surface roughness, surface elasticity, and surface motion on the development of adhesive forces in the interface. Our approach to discussing the recent literature on the topic of liquid-mediated adhesion is to organize things according to several basic characteristics: gross interface geometry (flat or curved), surface topography (smooth or rough), structural properties (rigid or deforming), meniscus type (constant-volume or constant-pressure) and separating process (quasi-static or dynamic). In this context, Table 1 categorizes recent research that is particularly relevant to the subject of this chapter. It is noted that an entry of "volume" under the "film constant" heading means that the volume of the liquid bridge is held fixed during the separation process, while an entry of "pressure" indicates that the liquid is assumed to remain in thermodynamic equilibrium with its vapor during the separation process.

Gross Interface Geometry	Surface Type	Deform. Behavior	Loading Process	Film Constant	Author(s)	Year Publ.	Ref. No.
flat on flat	smooth	elastic	quasi-static	volume	Zheng and Streator	2004	28
flat on flat	rough	elastic-plastic	quasi-static	pressure	Del Rio et al.	2008	19
flat on flat	rough	elastic	quasi-static	pressure	Wang and Regnier	2015	37
flat on flat	rough	elastic	quasi-static	pressure	Peng et al.	2009	21
flat on flat	rough	rigid	quasi-static	pressure or volume	de Boer and de Boer	2007	18
flat on flat	rough	elastically hard	quasi-static	pressure	de Boer	2007	17
flat on flat	rough	elastic	quasi-static	pressure	Persson	2008	20
flat on flat	rough	elastic	quasi-static	volume	Streator and Jackson	2009	34
flat on flat	rough	elastic	quasi-static	volume	Streator	2009	33
flat on flat	rough	elastic	quasi-static	volume	Rostami and Streator	2015	35

Gross Interface Geometry	Surface Type	Deform. Behavior	Loading Process	Film Constant	Author(s)	Year Publ.	Ref. No.
flat on flat	rough	elastic	quasi-static	volume	Rostami and Streator	2015	36
sphere on flat	smooth	elastic	quasi-static	pressure	Men et al.	2009	24
sphere on flat, and sphere on sphere	smooth	rigid	quasi-static	volume	Rabonivich et al.	2005	23
sphere on sphere	smooth	elastically soft	quasi-static	pressure	Butt et al.	2010	22
sphere on sphere	smooth	elastic	quasi-static	volume	Zheng and Streator	2003	30
sphere on sphere	smooth	elastic	quasi-static	volume	Zheng and Streator	2007	31
flat on flat	smooth	rigid	dynamic	n/a (flooded)	Roemer et al.	2015	15
flat on flat or sphere on flat	smooth	rigid	dynamic	volume	Cai and Bhushan	2007	9
sphere on flat	smooth	rigid	dynamic	n/a (flooded)	Streator	2006	25

Table 1. Recent research on the topic of the liquid-mediated adhesion

2. Models of solid surfaces bridged by a liquid

2.1. Liquid film between smooth, rigid, parallel flats

2.1.1. Static and quasi-static conditions

Consider the problem of a continuous liquid film that is at static equilibrium between two rigid, parallel flats in close proximity as shown in Figure 1. In this idealized case, the liquid forms an axisymmetric configuration, so that any horizontal cross section is circular. Because the liquid is in static equilibrium, the entire film must be at a single pressure. Per the Young-Laplace equation [8], the pressure drop Δp across the free surface is given by

$$\Delta p = p_a - p = \gamma\left(\frac{1}{R_1} + \frac{1}{R_2}\right). \tag{1}$$

Where p_a is the ambient pressure, p is the film pressure, and $R_{1,2}$ are the principal radii of normal curvature of the free surface at any given point on the free surface. Since we are dealing with small vertical spacing, it is reasonable to assume the radius of curvature (R_2) that exists in the plane of the figure at each free surface point is much smaller than the other principal radius of curvature (R_1), which lies in a plane that is perpendicular to the plane of the figure as well

as perpendicular to the tangent plane to the free surface at the point in question. In Figure 1, we have chosen to illustrate the value of R_1 that exists in the plane of minimum horizontal diameter. Assuming R_1 is sufficiently larger than R_2 that $1/R_1$ may be neglected, the pressure drop in Eq. (1) becomes

$$\Delta p = \frac{\gamma}{R_2} \tag{2}$$

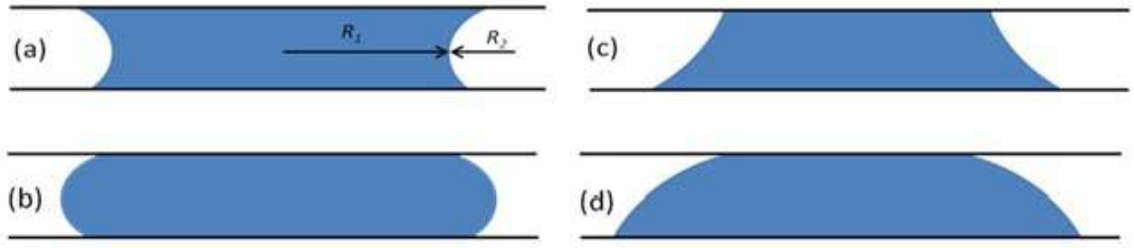

Figure 1. Profile of an axisymmetric liquid film between rigid, parallel plates. (a) The liquid wets both surfaces leading to a concave film shape. (b) The liquid wets neither surface, leading to a convex film shape. (c) The liquid wets one surface but not the other, with the wet surface closer to complete wetting than the non-wet surface is to complete non-wetting, leading to a convex film. (d) The liquid wets one surface, but not the other, with the non-wet surface closer to complete non-wetting than the wet surface is to complete wetting, leading to a convex film.

Moreover, owing to the fact that the liquid film, being continuous and in static equilibrium, must experience a uniform pressure, one may conclude that the radius of curvature R_2 is the same at every point of the free surface. Thus, the free surface profile is in the shape of a circle. Using this result leads to the geometrical relationship depicted in Figure 2, by which one concludes that

$$h = R_2(\cos\theta_1 + \cos\theta_2) \tag{3}$$

so that

$$\Delta p = \frac{\gamma(\cos\theta_1 + \cos\theta_2)}{h} \tag{4}$$

where $\theta_{1,2}$ are the liquid–solid contact angles. A liquid is considered to "wet" a given surface if its contact angle (measured from solid–liquid interface to the solid-vapor interface) is less than 90 degrees, and a liquid is considered to be non-wetting if its contact angle is greater than 90 degrees. Complete wetting is associated with a contact angle of 0 degrees and complete non-wetting corresponds to a contact angle of 180 degrees. While Figure 2 shows a case for which the liquid wets both upper and lower surfaces, Eq. (3) holds for each of the configurations depicted in Figure 1. Depending on both signs and relative magnitudes of the cosine terms in

http://dx.doi.org/10.5772/61572

Eq. (4), the film pressure may be greater than, equal to, or less than atmospheric pressure. For the case of Figure 1a, where both surfaces are wet by the liquid, both cosine terms are positive and the film pressure is sub-ambient. In contrast, for the case of Figure 1b, where neither surface is wet by the liquid, both cosine terms are negative and the film pressure exceeds the ambient pressure. When one of the surfaces is wet by the film while the other is not (Figures 1c and 1d), the sign of the film pressure depends on the relative magnitudes of the two cosine terms. When the contact angle associated with the surface that is wet by the liquid is closer to zero than the other contact angle is to 180 degrees (Figure 1c), then the film shape is concave and the film pressure is sub-ambient. On the other hand, if the contact angle associated with the surface that is wet by the liquid departs from zero degrees more than the opposing surface departs from 180 degrees (Figure 1d), then the film shape is convex and the film pressure is greater than ambient.

The value of the contact angle for a particular case is determined by a local thermodynamic equilibrium among the three relevant interfaces, which can be expressed in the Young-Dupree equation [8]

$$\gamma_{SV} = \gamma_{SL} + \gamma_{LV} \cos\theta \tag{5}$$

where γ_{SV}, γ_{SL} , and γ_{LV} are the surface energies per unit area of the solid–vapor, solid–liquid, and liquid–vapor interfaces, respectively. Note that γ_{LV} is the same as the surface tension of the liquid γ.

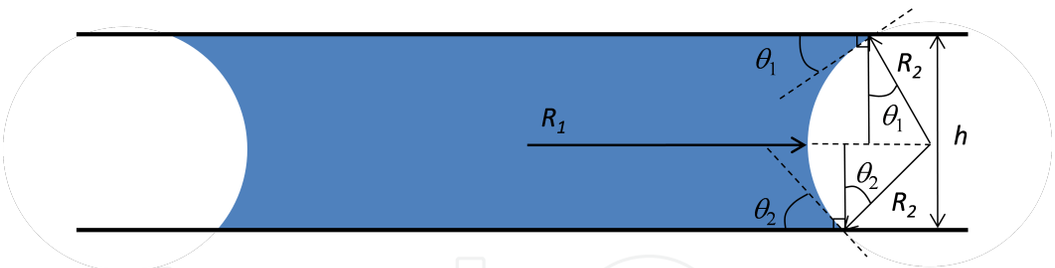

Figure 2. Geometrical relationship between plate spacing and radius of curvature of free surface for an assumed circular profile. Without loss of generality, the liquid is shown here as wetting both surfaces.

For a concave film shape (Figures 1a and 1c) the sum on the right-hand side of Eq. (4) is positive, yielding a positive pressure drop relative to atmospheric pressure. Thus, in terms of gauge pressure, the pressure within the film is negative. One important consequence is that the liquid exerts a force that pulls inward on the two plates so that the force exerted on either of the plates may be considered the force of adhesion due to the presence of the film. With reference to Figure 3, this adhesive force (F_{ad}) can be expressed as

$$F_{ad} = (-p)\pi R_1^2 + 2\pi R_1 \gamma = \frac{\gamma(\cos\theta_1 + \cos\theta_2)}{h}\ \pi R_1^2 + 2\pi R_1 \gamma \tag{6}$$

The first term on the right-hand side is the contribution to the adhesive force arising from the pressure drop across the free surface, while the second term is the adhesive force exerted by the free surface itself. Note that the total force exerted on the bottom of this upper section of the liquid film is simply transmitted to the upper plate, so the force given by Eq. (6) is indeed the adhesive force. Now under the assumption that R_1 is much greater than R_2, it can be shown that the force contribution to the pressure drop dominates the force contribution due to the free surface. Let the first term on the far right-hand side be denoted by $F_{\Delta p}$ and the second term be denoted by F_γ. Then $F_\gamma / F_{\Delta p} = 2\, R_2 / R_1$. Thus, to the extent that $1/R_1$ can be neglected in Eq. (1), which leads to Eq. (2), the force contributed by the free surface $2\pi R_1 \gamma$ may be neglected in Eq. (6).

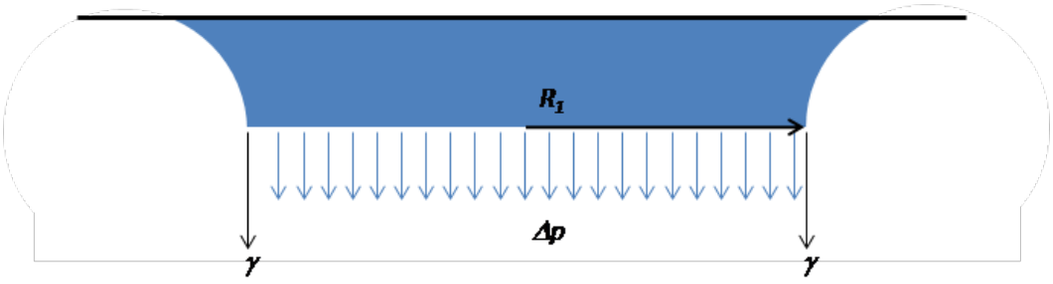

Figure 3. Sources of force exerted on the upper section of the fluid (dividing line chosen at the plane of minimum diameter).

Suppose now that the liquid film has a fixed volume V_o. To a good approximation, this volume may be expressed as $V_o = \pi R_1^2 h$, where the deviation from a cylindrical geometry has been ignored. Then the adhesive force may be written as:

$$F_{ad} = \frac{\gamma(\cos\theta_1 + \cos\theta_2)}{h^2} V_o \tag{7}$$

This equation shows that under the conditions of fixed liquid volume the adhesive force is inversely proportional to the square of the film thickness.

When a quantity of a pure liquid of given chemical species is at thermodynamic equilibrium, the partial pressure of the vapor phase of the species is equal to the vapor pressure of the liquid phase for the given temperature. For a curved free surface, there is a small deviation in the vapor pressure from that corresponding to a planar free surface. This deviation is accounted for by the well-known Kelvin equation [8]

$$ln\frac{p_s}{p_v} = \gamma\left(\frac{1}{R_1} + \frac{1}{R_2}\right)\frac{V_m}{RT} = \frac{\gamma}{R_K}\frac{V_m}{RT} \tag{8}$$

where p_s is the saturation pressure at the given temperature, p_v is the pressure of the vapor just outside of the liquid film, V_m is the molar volume, R_K is the Kelvin radius, R is the universal

http://dx.doi.org/10.5772/61572

gas constant, and T is the absolute temperature. Assuming, as before, $R_1 \gg R_2$, and then isolating R_2, one obtains

$$R_2 = R_K = -\frac{\gamma V_m}{RT\ln\frac{p_v}{p_s}} \tag{9}$$

Using this result in Eq. (2) gives

$$p_a - p = -\frac{RT\ln\frac{p_v}{p_s}}{V_m} \tag{10}$$

Now, suppose the chemical species in question is water, so that the ratio p_v / p_s represents the relative humidity. Then Eq. (9) states that, at thermodynamic equilibrium, the radius of curvature of any free surface of the liquid film is determined by the relative humidity. For example, taking properties of water at room temperature and assuming a relative humidity of 95%, we have

$$R_2 = -\frac{\left(0.0727\frac{\mathrm{N}}{\mathrm{m}}\right)\left(0.018\ \mathrm{kg/mol}\right)/\left(.00100\mathrm{m}^3/\mathrm{kg}\right)}{8.314\frac{\mathrm{J}}{\mathrm{mol-K}}\left(293\mathrm{K}\right)\ln\left(0.95\right)} = 10.5\,\mathrm{nm} \tag{11}$$

so that, from Eq. (10),

$$p_a - p = -\frac{RT\ln\frac{p_v}{p_s}}{V_m} = \frac{\left(0.0727\frac{\mathrm{N}}{\mathrm{m}}\right)}{10.5\ \mathrm{nm}} = 6.9\ \mathrm{MPa} \tag{12}$$

If we take the contact angles to be zero, then, from Eq. (4) and Eq. (11), $h = 2R_2 = 21$ nm. Now, for this mathematically idealized case of perfectly parallel plates, 21 nm would be the only spacing for which a liquid film could exist at thermodynamic equilibrium at 95% relative humidity. On the other hand, if the surfaces were curved, even slightly, then there would be a range of humidity values for which a film could be sustained at thermodynamic equilibrium. It should be noted that, in practical situations, the establishment of thermodynamic equilibrium may require a considerable amount of time, such as hours, or even days. In the interim, the adhesive forces will be dictated by the current amount of liquid within the interface.

2.1.2. Dynamic separation

The foregoing analysis is applicable to conditions of static (or quasi-static) equilibrium. Additional effects may arise from viscous interactions. Consider now a situation where the upper plate is pulled upward at a prescribed rate, while the lower plate is held fixed. One approach to analyzing such a situation [9] is to assume that the liquid flow is governed by the Reynolds equation of lubrication [10].

$$\frac{1}{r}\frac{\partial}{\partial r}\left(rh^3\frac{\partial p}{\partial r}\right)=12\mu\frac{\partial h}{\partial t} \tag{13}$$

where r is the radial coordinate measured from the center of the axisymmetric film cross-section. Assuming that the gap, h, is uniform (i.e., independent of r), the above equation can be integrated twice to give

$$p(r,t)=3\mu\frac{\dot{h}}{h^3}+c_1(t)\ln(r)+c_o(t) \tag{14}$$

where $\dot{h}\equiv\frac{\partial h}{\partial t}$ and $c_1(t)$ and $c_o(t)$ are constants of integration (i.e., independent of r).

To obtain the constants of integration, we assume that (1) the pressure just inside the free surface is that corresponding to the static case (see Eq. 4), and (2) the pressure is finite at $r = 0$. Then letting R_1, as before, denote the inner radius of the droplet, we obtain (in terms of gauge pressure):

$$p(r,t)=-\frac{\gamma(\cos\theta_1+\cos\theta_2)}{h}+3\mu\frac{\dot{h}}{h^3}\left(r^2-R_1^2\right) \tag{15}$$

Now, the adhesive force is just given by

$$F_{ad}=\int_0^b -p(r,t)2\pi r dr=\frac{\gamma(\cos\theta_1+\cos\theta_2)}{h}\pi R_1^2+\frac{3}{2}\pi\mu\frac{\dot{h}}{h^3}R_1^4 \tag{16}$$

For a fixed liquid volume (V_o), which is approximated by $V_o=\pi R_1^2 h$, we arrive at

$$F_{ad}=\int_0^b -p(r,t)2\pi r dr=\frac{\gamma(\cos\theta_1+\cos\theta_2)}{h^2}V_o+\frac{3}{2}\mu\frac{\dot{h}}{h^5}V_o^2 \tag{17}$$

http://dx.doi.org/10.5772/61572

The above equation shows that adhesive force grows in proportion to the rate $\dot{h}$ at which the plates are being pulled apart and is quite sensitive to the value of separation. Small separations require a much larger separating force than what is required at larger separations for the given separating rate. One caveat, however, is that there is a practical limit as to the magnitude of negative pressure that can be sustained during the separation of surfaces. Whereas thermodynamic equilibrium suggests that the liquid will cavitate once its absolute pressure approaches zero (e.g., [11]), it has also been found that, in certain cases, the liquid film may achieve absolute pressures that are negative [7, 12–15]. For example, an analytical model was developed [15] for the dynamic vertical separation of opposing plates and, based on fitting with experimental data, a tensile strength of 35 kPa was found for a mineral oil. In any case, if one denotes p_{cav} as the cavitation pressure (relative to atmospheric pressure), then the maximum possible adhesive force can be written as:

$$F_{ad} = -p_{\text{cav}} \pi R_1^2 \tag{18}$$

2.2. Liquid film between rigid, inclined surfaces

Consider the situation depicted in Figure 4, where there is a liquid film between two flat surfaces whose planes intersect. The configuration of Figure 4a is a non-equilibrium state owing to the greater free-surface curvature on the right than on the left, and the associated lower pressure (i.e., greater reduction in pressure compared to ambient). Thus, the fluid will flow from left to right, all the way up to the edge (Figure 4b) until achieving a configuration with equal free-surface curvature at left and right ends, thereby yielding the same pressure drop. The two-dimensional depiction of Figure 4, of course, obscures the required re-configuration that happens in three dimensions. In fact, the entire free surface must attain the same curvature, which means that liquid would find its way to both the front and back edges as well as the right edge.

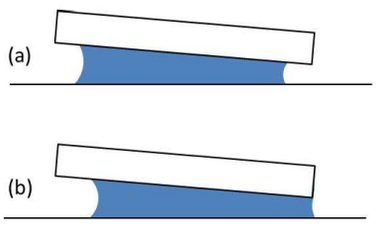

Figure 4. Liquid film between inclined surfaces: (a) non-equilibrium configuration and (b) equilibrium configuration.

2.3. Liquid film between a smooth, rigid sphere and a rigid flat

The sphere-flat configuration is of interest in its own right and as an important part of a rough surface contact model, in which contributions from various asperity-asperity liquid bridges are summed by viewing each pair as reflecting the interaction between a pair of spheres having the asperity curvatures.

2.3.1. Static and quasi-static conditions

The interaction between a sphere and flat bridged by a liquid film, as illustrated in Figure 5, has been analyzed in [16]. When the radial width of the liquid film (b) is sufficiently small compared to the radius of the sphere, the slope of the sphere at the location of the free surface may be taken as horizontal. In this case, the pressure within the film will be given by Eq. (4) with h replaced by $h(b)$, the film thickness at the radial location of the free surface. Additionally, the sphere contour can be approximated well by that of a paraboloid, so that

$$h(b) = D + \frac{b^2}{2R} \tag{19}$$

This gives

$$p_a - p = \frac{\gamma(\cos\theta_1 + \cos\theta_2)}{h(b)} = \frac{\gamma(\cos\theta_1 + \cos\theta_2)}{D + \dfrac{b^2}{2R}} \tag{20}$$

The force of adhesion is obtained by multiplying this pressure difference by the cross-section area of the liquid bridge (πb^2), giving (after re-arrangement)

$$F_{ad} = 2\pi R\gamma(\cos\theta_1 + \cos\theta_2)\left(1 - \frac{D}{h(b)}\right) = \frac{2\pi R\gamma(\cos\theta_1 + \cos\theta_2)}{1 + \dfrac{2RD}{b^2}} \tag{21}$$

Several studies have considered the role of relative humidity on the adhesion between a sphere and a flat (or sphere on sphere) [9, 17–23], where, at thermodynamic equilibrium, the radius of the curvature of the free surface of the meniscus would be equal to the Kelvin radius, per Eq. (9). Such analysis is most appropriate for volatile liquids [24]. In this case the value of $h(b)$ appearing in Eq. (21) would be determined directly by the relative humidity, via Eqs. (3) and (9).

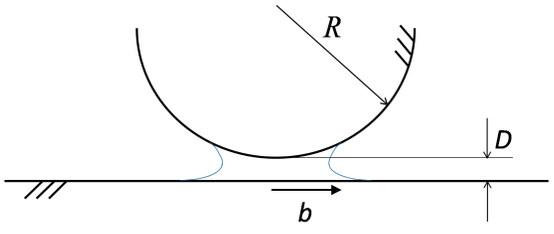

Figure 5. Liquid film between a rigid sphere and a rigid flat.

http://dx.doi.org/10.5772/61572

2.3.2. Dynamic separation

Now we consider the forces that arise when a sphere of mass m and radius R is separated from the flat in a dynamic fashion, so that the minimum spacing D is a function of time. Denoting the instantaneous vertical spacing between the sphere surface and the flat as $h(r, t)$, we have $D=h(0, t)$. When the wetted radius b is much smaller than the sphere radius, one gets

$$h(r,t) = D(t) + \frac{r^2}{2R} \tag{22}$$

When a net external force F (i.e., an applied force less the sphere weight) acts on the sphere (positive upward), the governing equation becomes [25]

$$m\frac{d^2D}{dt^2} = F - F_m - F_v \tag{23}$$

where F_m is the "meniscus" force, which accounts for the effect of the pressure drop across the curved free surface of the liquid meniscus and F_v is the "viscous" force, which arises from the deformation of the liquid bridge. It is assumed that any buoyancy forces are negligible. Following [26], the pressure field, as derived from the solution of the Reynolds equation (e.g., [10]), can be written as

$$p(r,t) = p(b,t) - 3\mu R\left(\frac{1}{h(r,t)^2} - \frac{1}{h(b,t)^2}\right)\frac{1}{D}\frac{dD}{dt} \tag{24}$$

where μ is the liquid viscosity. Note that the wetted radius b is itself a function of time. Assuming that the free surface of the liquid has the same shape as when the film is quasi-static, the pressure just inside the meniscus, $p(b, t)$ is given by Eq. (4). Thus, integrating over the meniscus area gives [25]

$$F_{ad} = F_m + F_v = 2\pi R\gamma(\cos\theta_1 + \cos\theta_2)\left(1 - \frac{D}{h(b,t)}\right) + 6\pi\mu R^2\left(1 - \frac{D}{h(b,t)}\right)^2\frac{1}{D}\frac{dD}{dt} \tag{25}$$

where F_{ad} is the adhesive force. Direct integration of the film thickness profile (19) provides the liquid volume:

$$V = \pi b^2 D + \frac{\pi b^4}{4R} = \pi R\left[h(b,t)^2 - D^2\right] \tag{26}$$

Assuming the meniscus volume is fixed, we set $V = V_o$ and express the film thickness at the free surface as

$$h(b,t) = \sqrt{D^2 + \frac{V_o}{\pi R}} \tag{27}$$

Using this result in Eq. (25) allows the force exerted by the liquid to be expressed in terms of the separation D

$$F_{ad} = F_m + F_v = 2\pi R\gamma(\cos\theta_1 + \cos\theta_2)\left(1 - \frac{D}{\sqrt{D^2 + \frac{V_o}{\pi R}}}\right) + 6\pi\mu R^2\left(1 - \frac{D}{\sqrt{D^2 + \frac{V_o}{\pi R}}}\right)^2 \frac{1}{D}\frac{dD}{dt} \tag{28}$$

In cases where the inertial term of Eq. (23) is negligible, the net applied load F is equated with the sum of the capillary and viscous forces F_{ad}. Moreover, in cases where the variation in the capillary force is small compared to the variation in the viscous force, Eq. (28) can be integrated to give [9, 27]

$$\int_0^{t_s}\left(F - F_m\right)dt = \int_0^{D_s} F_v dt = \int_0^{D_s} F_v \frac{dt}{dD}dD = 6\pi\mu R^2 ln\left[\frac{D_s\left(D_o + \sqrt{D_o^2 + \frac{V_o}{\pi R}}\right)^2\sqrt{D_s^2 + \frac{V_o}{\pi R}}}{D_o\left(D_s + \sqrt{D_s^2 + \frac{V_o}{\pi R}}\right)^2\sqrt{D_o^2 + \frac{V_o}{\pi R}}}\right] \tag{29}$$

where t_s is the time to completely separate the surfaces, D_s is the distance at which the sphere and flat are considered completely separated, and D_o is the sphere-flat spacing at the beginning of the separation process. It was argued in [27] that even in the case of initial solid-solid contact, the value of D_o should not be zero, but should be selected in accordance with the interface roughness. Eq. (29) suggests that the separation process for a viscous-dominated interaction is governed by the time integral of the viscous force, known as the viscous impulse, the value of which is a function only of the input parameters of the problem [27]. Now the distance of complete separation D_s is taken as infinite in [27], and finite in [9]. For $D_s \to \infty$, Eq. (29) can be simplified [27], giving

$$I_v = 6\pi\mu R^2 ln\left[\frac{\left(D_o + \sqrt{D_o^2 + \frac{V_o}{\pi R}}\right)^2}{4D_o\sqrt{D_o^2 + \frac{V_o}{\pi R}}}\right] = 6\pi\mu R^2 ln\left[\frac{\left(D_o + \sqrt{D_o^2 + \frac{V_o}{\pi R}}\right)^2}{4D_o\sqrt{D_o^2 + \frac{V_o}{\pi R}}}\right] \tag{30}$$

where I_v is the viscous impulse. Applying Eq. (30) to the case of a sphere interacting with a surface that is initially covered with a thin film of uniform thickness h_o, the above is approximated by [27]

$$I_v = 6\pi\mu R^2 \ln\left(h_o / 2D_o\right) \tag{31}$$

One important result of the above relationship is that the rate of applied loading determines the peak adhesive load developed during separation, which we label here the "pull-off force" ($F_{\text{pull-off}}$).

For example, when the externally applied force increases at a constant rate ($\dot{F}$), the pull-off force takes the form:

$$F_{\text{pull-off}} = F_m + \sqrt{2\dot{F}I_v} \tag{32}$$

A modified approach is needed to analyze the "fully-flooded" case, where the sphere interacts with a sufficiently thick lubricant film that further increases to the film thickness have negligible impact on the adhesive force. In this case, Eq. (32) still holds, but the viscous impulse becomes [25]

$$I_v = 6\pi\mu R^2 \ln\left[0.1\frac{\left(6\pi\mu R^2\right)^{\frac{3}{2}}}{mD_o\sqrt{2\dot{F}}}\right] \tag{33}$$

where m is the mass of the sphere.

It is emphasized here that Eqs. (28)-(33) presume the liquid film is not experiencing any cavitation. As discussed previously (see Eq. (18)), the potential development of a fully cavitated film would provide an upper bound for the adhesive force.

2.4. Liquid film between smooth, elastic flats

Figure 6 depicts a scenario when a liquid film interacts with two semi-infinite elastic bodies, where $E_{1,2}$ and $\nu_{1,2}$ are the elastic moduli and Poisson ratios of bodies 1 and 2, respectively and H is the uniform gap between the surfaces that exists in the absence of deformation. For this situation, the pressure within the liquid film causes elastic deformation of the half-spaces. Here we focus our attention on the case were the liquid film wets both surfaces such that they each experience a contact angle less than 90 degrees. This problem has been analyzed previously [28] and that work is summarized here. Letting Δp represent the pressure drop across the free surface of the liquid (from outside to inside), the film pressure (gauge) can be expressed as

$$p(r)=\begin{cases}-\Delta p & r\le b\\ 0 & r>b\end{cases} \tag{34}$$

This pressure field causes an associated deformation field [29]

$$u(r)=u_1(r)+u_2(r)=\begin{cases}\dfrac{4\Delta pb}{\pi E'}\displaystyle\int_0^{\pi/2}\sqrt{1-\frac{r^2}{b^2}\sin^2\psi}\,d\psi & r\le b\\ \dfrac{4\Delta pb}{\pi E'}\displaystyle\int_0^{\pi/2}\frac{b^2\cos^2\psi}{\sqrt{1-\frac{r^2}{b^2}\sin^2\psi}}\,d\psi & r>b\end{cases} \tag{35}$$

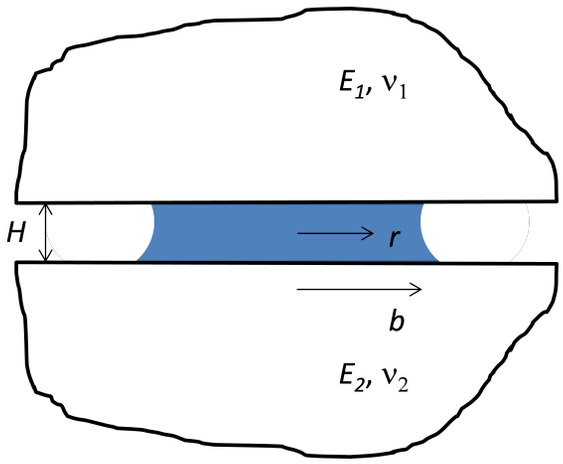

Figure 6. A liquid film bridging two elastic half-spaces.

In the above equation, $u_1(r)$ and $u_2(r)$ are the normal surface displacements of bodies 1 and 2, respectively (each positive toward the opposing body), $u(r)$ is the total displacement, and the reduced modulus E' is given by $1/E'\equiv(1-\nu_1^2)/E_1+(1-\nu_2^2)/E_2$. It is assumed here that the bulk positions of the bodies are fixed, so that opposing surface points remote to the interface are maintained at a spacing of H. At any radial position within the wetted film, the film thickness can be expressed as

$$h(r)=H-u(r) \tag{36}$$

Using Eq. (35), the volume of the liquid bridge (V_o), which is assumed to be fixed, is given by

$$V_o=\int_o^b 2\pi rh(r)\,dr=\pi Hb^2-\frac{16}{3E'}\Delta pb^3 \tag{37}$$

http://dx.doi.org/10.5772/61572

The equilibrium configuration can be determined by considering the minimization of the free energy, which is comprised of elastic strain energy (U_S) and surface energy U_E. The elastic strain energy is simply given by the work done in creating the deformation field

$$U_E = \frac{1}{2}\int_o^b \Delta p u(r) 2\pi r dr \tag{38}$$

Using Eq. (35) and carrying out the integration gives

$$U_E = \frac{8}{3E'}\Delta p^2 b^3 \tag{39}$$

Now the surface energy consists for energy contributions from the solid-vapor, solid-liquid, and liquid-vapor interfaces, so that

$$U_S = \pi\left(R_o^2 - b^2\right)\left(\gamma_{SV_1} + \gamma_{SV_2}\right) + \pi b^2\left(\gamma_{SL_1} + \gamma_{SL_2}\right) + A_{LV}\gamma \tag{40}$$

where subscripts 1 and 2 refer to the upper and lower surfaces, respectively and R_o is the radius of an arbitrary control region that encloses the interface. It is reasonable to assume here that the film thickness at the free surface is sufficiently small compared to the meniscus radius that the energy contributions from the liquid-vapor interface are negligible. Then the total free energy is given by

$$U_T = U_S + U_E = \pi\left(R_o^2 - b^2\right)\left(\gamma_{SV_1} + \gamma_{SV_2}\right) + \pi b^2\left(\gamma_{SL_1} + \gamma_{SL_2}\right) + \frac{8}{3E'}\Delta p^2 b^3 \tag{41}$$

Applying Eq. (5) to each surface and recalling that $\gamma \equiv \gamma_{LV}$ one obtains

$$U_T = \pi R_o^2\left(\gamma_{SV_1} + \gamma_{SV_2}\right) - \pi b^2\gamma\left(\cos\theta_1 + \cos\theta_2\right) + \frac{8}{3E'}\Delta p^2 b^3 \tag{42}$$

A stable equilibrium corresponds to the minimization of the free energy U_T under the constraint of constant liquid volume V_o. Let us now introduce dimensionless quantities:

$$\eta \equiv \frac{2\Delta pb}{E'H} \tag{43}$$

$$U_T^* \equiv \frac{U_T - \pi R_o^2\left(\gamma_{SV_1} + \gamma_{SV_2}\right)}{\sqrt{\pi}E'H^{3/2}V_o^{1/2}} \tag{44}$$

$$\Gamma \equiv \frac{\gamma^2\left(\cos\theta_1 + \cos\theta_2\right)^2 V_o}{4E'^2H^5} \tag{45}$$

With these definitions, the dimensionless free energy can be expressed as

$$U_T^* \equiv \frac{2\eta^2}{3\pi\sqrt{1-\left(8/3\pi\right)\eta}} - 2\sqrt{\frac{\Gamma}{\pi}}\frac{1}{1-\left(8/3\pi\right)\eta} \tag{46}$$

Note also that from Eqs. (35), (36) and (43), the minimum film thickness is given by

$$h_{\min} = H - u\left(0\right) = H - \frac{2\Delta pb}{E'} = H\left(1-\eta\right) \tag{47}$$

So that η provides a dimensionless measure as to the degree of surface approach. When $\eta = 0$, the surfaces are at the original separation throughout, and when $\eta = 1$ the surfaces come into point contact. For a stable equilibrium, the dimensionless energy achieves a local minimum with respect to η. Thus, a necessary (but not sufficient) condition for stable equilibrium is that $dU_T^*/d\eta = 0$, which yields the following requirement:

$$\eta^2\left(1-\frac{2}{\pi}\eta\right)^2\left(1-\frac{8}{3\pi}\eta\right) = \frac{16\Gamma}{\pi} \tag{48}$$

The solution space of Eq. (48) is shown in Figure 7. An investigation of $d^2U_T^*/d\eta^2$ at the various equilibrium values of η reveals that values to the left of the peak ($\eta < 0.5577$) correspond to stable equilibrium configurations, whereas those to the right of the peak, correspond to unstable equilibrium configurations. From the graph, we see that no equilibrium configurations exist for values of Γ greater than 0.0134. This result implies that solid-solid contact must occur whenever $\Gamma > 0.0134$. Further, once solid-solid contact occurs, the contact region grows without bound (i.e., the free energy, which now includes a solid-solid contribution, decreases monotonically with increasing contact radius).

http://dx.doi.org/10.5772/61572

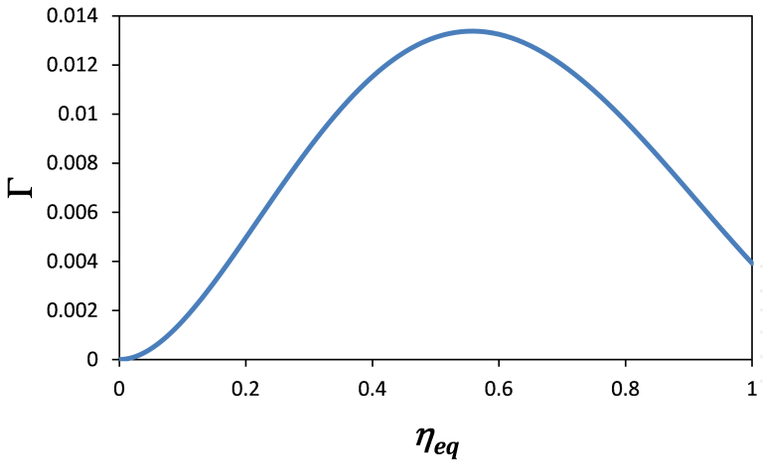

Figure 7. Equilibrium configurations for two half-spaces bridged by a liquid film.

Using Figure 7, one can determine the adhesive force. Letting the subscript "eq" identify values corresponding to a stable equilibrium configuration, it can be shown using Eqs. (35)–(37), (43), and (48), that

$$b_{eq} = \sqrt{\frac{V_o}{\pi H\left(1-\frac{8}{3\pi}\eta_{eq}\right)}} \tag{49}$$

$$h_{eq}(b_{eq}) = H\left(1-\frac{2}{\pi}\eta_{eq}\right) \tag{50}$$

$$\Delta p_{eq} = \frac{\gamma(\cos\theta_1+\cos\theta_2)}{h_{eq}(b_{eq})} \tag{51}$$

Then, the adhesive force is given by

$$F_{ad} = \pi b_{eq}^2 \Delta p_{eq} = \frac{\gamma(\cos\theta_1+\cos\theta_2)V_o}{H^2\left(1-\frac{8}{3\pi}\eta_{eq}\right)\left(1-\frac{2}{\pi}\eta_{eq}\right)} \tag{52}$$

2.5. Liquid film between smooth, elastic spheres

When a liquid bridges two elastic spheres [30], as illustrated in Figure 8, the situation is similar to the case of two elastic half-spaces (discussed above), but with an added feature due the

surface curvature. The displacement profile is still given by Eq. (35), but the film thickness profile is now given by

$$h(r) = H + \frac{r^2}{2R} - u(r) \tag{53}$$

where R is the composite radius of curvature, defined by $1/R = 1/R_1 + 1/R_2$. Thus, upon integrating, the liquid volume takes the form

$$V_o = \pi H b^2 - \frac{16}{3E'}\Delta p b^3 + \frac{\pi b^4}{4R} \tag{54}$$

Note that the expressions for the elastic strain energy and surface energy are the same as those for the two half-spaces, so that the total free energy is still given by Eq. (41). In addition to non-dimensional parameters η and Γ (Eqs. 43 and 45), we introduce a dimensionless volume according to

$$\Psi \equiv \frac{V_o}{RH^2} \tag{55}$$

and use a different form for the dimensionless free energy

$$U_T^* \equiv \frac{U_T - \pi R_o^2\left(\gamma_{SV_1} + \gamma_{SV_2}\right)}{\pi E' H^{5/2} R^{1/2}} \tag{56}$$

This results in

$$U_T^* = 4\sqrt{\frac{\Gamma}{\pi}}\left[1 - \frac{8}{3\pi}\eta - \sqrt{\left(1 - \frac{8}{3\pi}\eta\right)^2 + \frac{\Psi}{\pi}}\right] + \frac{2}{3\pi}\eta^2\sqrt{-2\left(1 - \frac{8}{3\pi}\eta\right) + \sqrt{\left(1 - \frac{8}{3\pi}\eta\right)^2 + \frac{\Psi}{\pi}}} \tag{57}$$

Setting $dU_T^*/d\eta = 0$ leads to the following necessary condition on η for a stable equilibrium to be achieved

$$\eta^2\left[\frac{2}{3\pi}\eta + \sqrt{\left(1 - \frac{8}{3\pi}\eta\right)^2 + \frac{\Psi}{\pi}}\right]^2\left[1 - \frac{8}{3\pi}\eta + \sqrt{\left(1 - \frac{8}{3\pi}\eta\right)^2 + \frac{\Psi}{\pi}}\right] = \frac{32\Gamma}{\pi} \tag{58}$$

http://dx.doi.org/10.5772/61572

It can readily be shown that for $\Psi=0$, Eq. (58) reduces to Eq. (48), which is applicable to two half-spaces. This result is expected because for a finite liquid volume and a finite, non-zero value of surface spacing, an infinite value of sphere radius (which corresponds to a flat-flat interface) causes Ψ to vanish as per Eq. (55).

The solution space for Eq. (58) is plotted in Figure 9 for several values of dimensionless volume Ψ. As observed, the smallest chosen value of Ψ yields a curve that is quite close to the half-space solution (Figure 7). It turns out that stable equilibrium configurations exist without solid-solid contact for a range of Γ values that depends on the value of Ψ. This relationship is summarized in Figure 10, which reveals regions with and without solid-solid contact within $\Psi-\Gamma$ space. The boundary curve is given by $\Gamma_c=0.03007\Psi^{1.3955}+0.01336$. If, for a given Ψ, $\Gamma<\Gamma_c$ then there is no solid-solid contact, whereas for $\Gamma\geq\Gamma_c$ the spheres must experience contact.

For equilibrium configurations that do not involve solid-solid contact, the pressure drop is given by Eq. (51), but with the gap at the free-surface given by

$$h_{eq}(b_{eq})=H\left[\frac{2}{3\pi}\eta_{eq}+\sqrt{\left(1-\frac{8}{3\pi}\eta_{eq}\right)^2+\frac{\Psi}{\pi}}\right] \tag{59}$$

and the wetted radius given by (via solution of Eq. 54)

$$b_{eq}=\left\{\frac{2V_o}{\pi H\left[1-\frac{8}{3\pi}\eta_{eq}+\sqrt{\left(1-\frac{8}{3\pi}\eta_{eq}\right)^2+\frac{V_o}{\pi RH^2}}\right]}\right\}^{\frac{1}{2}} \tag{60}$$

.

Thus, the adhesive force then becomes

$$F_{ad}=\pi b_{eq}^2\Delta p_{eq}=\frac{2\gamma(\cos\theta_1+\cos\theta_2)V_o}{H^2\left[1-\frac{8}{3\pi}\eta_{eq}+\sqrt{\left(1-\frac{8}{3\pi}\eta_{eq}\right)^2+\frac{V_o}{\pi RH^2}}\right]\left[\frac{2}{3\pi}\eta_{eq}+\sqrt{\left(1-\frac{8}{3\pi}\eta_{eq}\right)^2+\frac{\Psi}{\pi}}\right]} \tag{61}$$

The above force represents the external, separating force (over and above the weight of the sphere) required to maintain the spheres at the given configuration (i.e., with undeformed separation, H).

In cases where $\Gamma > \Gamma_c$, the solids come into contact over some contact radius a, with the contact region surrounded by an annulus of liquid. The presence of contact modifies the form of the free energy, which becomes [31]

$$U_T = \pi\left(R_o^2 - b^2\right)\left(\gamma_{SV_1} + \gamma_{SV_2}\right) - \pi\left(b^2 - a^2\right)\left(\gamma_{SL_1} + \gamma_{SL_2}\right) + \pi a^2 \gamma_{S_{12}} \tag{62}$$

where $\gamma_{S_{12}}$ is the surface tension associated with the solid-solid interface.

The dimensionless formulation involves two additional ratios [31]:

$$m \equiv \frac{b}{a} \tag{63}$$

$$\Phi \equiv \frac{\Delta\gamma}{\gamma\left(\cos\theta_1 + \cos\theta_2\right)} - 1 \tag{64}$$

where $\Delta\gamma$ is the well-known work of adhesion and is given by [8]

$$\Delta\gamma = \gamma_{SV_1} + \gamma_{SV_2} - \gamma_{S_{12}} \tag{65}$$

The equilibrium solution, for given values of Γ and Ψ, is now expressed in terms of both η and m. In the case of solid-solid contact, no analytical expressions exist for the elastic strain energy, owing to the unknown contact solid-solid pressure distribution. Therefore, the equilibrium configurations and associated adhesive forces must be acquired through a numerical process [31].

It can be shown [31] that the advent of solid-solid contact introduces hysteresis, just as in the case of the JKR contact model [32], which applies to dry contact. Thus, the set of configurations that the interface would pass through when breaking the contact, such as during a controlled separation process, would be different from those experienced upon its formation. For example, the value of H at which the solid-solid contact is lost during a separation process is different from the value of H that corresponds to the formation of solid-solid contact during an approach process. Put another way, there is a jump-on instability at a certain H upon approach, where the interface goes suddenly from no contact to contact, as well as a jump-off instability upon separation (at a larger H), where the interface proceeds suddenly from having a contact radius a to having no solid-solid contact. One convenient experimental measure of the strength of an adhesive contact is the pull-off force, which can take on different values

http://dx.doi.org/10.5772/61572

depending upon how the pull-off process is conducted. When the separation H (which is defined by the minimum gap between the undeformed sphere contours) is specified and increased quasi-statically, the interface will reach a configuration that is unstable and then abruptly lose contact. The magnitude of external, separating force required to reach this point of instability during separation is defined as the pull-off force during a controlled separation process.

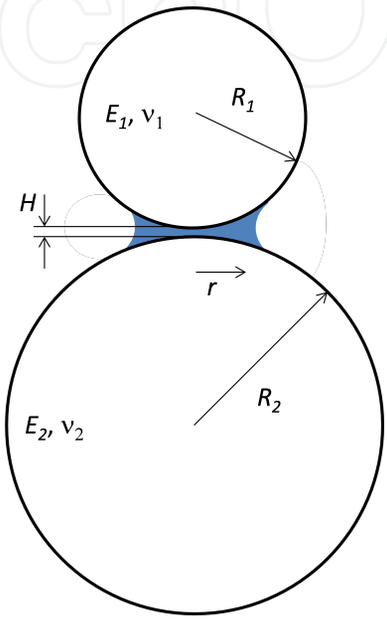

Figure 8. A liquid film bridging two smooth, elastic half-spaces with no solid-solid contact.

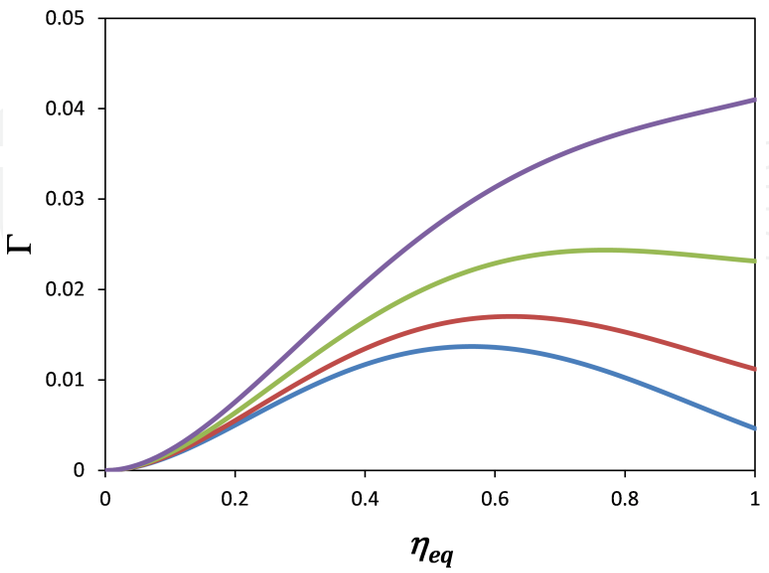

Figure 9. Equilibrium configurations for two spheres bridged by a liquid film without solid-solid contact.

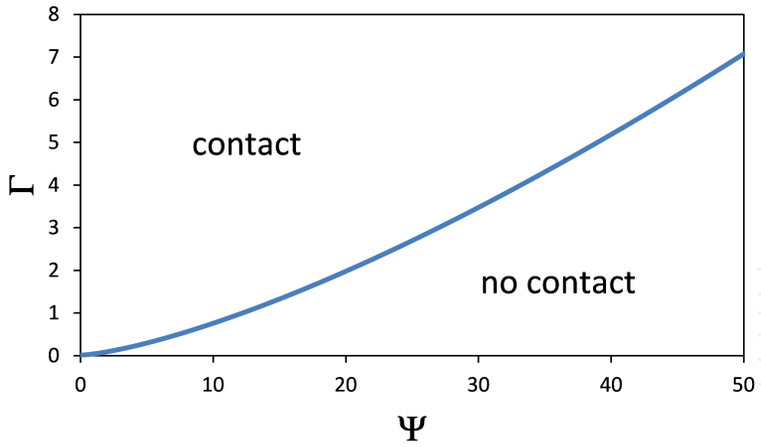

Figure 10. Regions in Γ-Ψ space showing regions with and without solid-solid contact.

2.6. Liquid film between contacting rough, elastic surfaces

Adhesive forces arising due to the presence of a liquid film between rough, elastic (or elastic-plastic) surfaces have been the subject of several recent works [17, 19–21, 33–37]. Figure 11 depicts a situation where two rough, elastic surfaces are in contact in the presence of an intervening liquid film. Taking into consideration a three-dimensional geometry, the assumption here is that the liquid film is continuous, so that there are no regions of liquid completely encased within a zone of solid-solid contact. Now in the case where the liquid wets the surfaces (i.e., the contact angles are less than 90°), the free surface of the liquid is concave and the film pressure is sub-ambient. Assuming that the lateral dimensions are much greater than the liquid film thickness, the pressure drop across the free surface is given by

$$\Delta p = p_a - p = \frac{\gamma(\cos\theta_1 + \cos\theta_2)}{h_{fs}} \tag{66}$$

where h_{fs} is the film thickness at the location of the free surface. For a continuous liquid film in static equilibrium, the pressure throughout the film must be the same, so Eq. (66) suggests that the periphery of the liquid film is at a constant height. The overall equilibrium shape of the film will depend upon the details of the gap distribution within the surfaces, which itself will be modulated by surface deformation due to the tensile stresses exerted by the liquid film. In general, the equilibrium configuration of the liquid film will not be axisymmetric. However, for surfaces that are nearly flat aside from a small-scale roughness, we can expect that the equilibrium film shape will be nearly axisymmetric. Assuming an axisymmetric liquid film, one can describe the establishment of equilibrium as follows: First, suppose a quantity of liquid is placed upon a surface that will serve as the lower surface of the contacting pair. Then, the other surface is placed in contact with the lower surface (and the liquid film) under some external load P. As solid-solid contact is first formed at the mutual asperity peaks, the liquid

film will be quickly squeezed out to a radius that is determined by the given liquid volume and the average gap between the surfaces within the wetted region. However, as capillary forces take effect, the elastic surfaces will further deform, thereby reducing the mean gap between the surfaces and causing an increase in the wetted radius. An increase in the wetted radius in conjunction with a decreasing interfacial gap will cause a greater tensile force F_t and greater surface deformation. Hence, there is the possibility that the rate of increase of the capillary force (with expanding wetted radius) will exceed the rate of increase of the compressive force coming from the contacting asperities. In such a situation, the interface is expected to collapse, whereby the solid surfaces come into complete or nearly complete contact.

One numerical model of such an interface appears in [35]. Here it is assumed that the liquid film is axisymmetric and that deformation of the asperities is modeled according to the multi-scale contact model of [38]. Thus, the surface topography is characterized by its spectral content and algebraic formulas are applied to compute the effects of external and capillary forces on the average spacing within the interface. Another important assumption is that the mean spacing $\bar{h}$ within the wetted region is a good approximation to the spacing at the free surface h_{fs} so that pressure drop within the film is approximated by

$$\Delta p = \frac{\gamma(\cos\theta_1 + \cos\theta_2)}{\bar{h}} \tag{67}$$

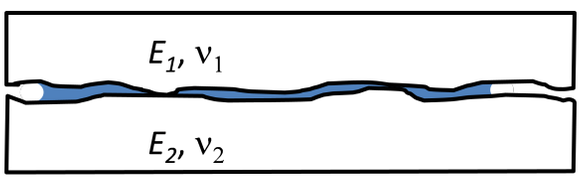

Figure 11. A liquid film bridging two rough, elastic surfaces.

Thus, the tensile force (F_t) becomes

$$F_t = \pi b^2 \frac{\gamma(\cos\theta_1 + \cos\theta_2)}{\bar{h}} \tag{68}$$

where b is the radius of the wetted region. If one defines the adhesive force as the tensile contribution to the net force exerted on either solid body, then F_t is the just the adhesive force (F_{ad}). An alternative definition for the adhesive force would be the value of the tensile external load required to maintain static equilibrium, or required to achieve a certain separation and

separation rate. The latter definition views the adhesive force as the interfacial tensile force less the interfacial compressive force.

Sample results of the analysis are displayed in Figure 12, for the following input parameters: $V_o = 0.1$ mm^3, $\gamma = 72.7$ mN/m, $\sigma = 0.4$ μm, and $A_n = 4$ cm^2, where σ is the r.m.s. surface roughness of a 3D isotropic surface with a Gaussian height distribution, and A_n is the nominal contact area of the interface (i.e., the projected area of the interface in Figure 11). Figure 12 shows the influence of external load on several contact parameters, including tensile force and contact area (Fig. 12a) as well as average gap and wetted radius (Fig. 12b). The tensile force is seen to grow steadily with increasing external load until approaching a critical load, where the rate of increase of tensile force with load approaches infinity. The attainment of a near vertical slope in the curve suggests that the interface is unstable: no equilibrium configurations could be found for values of external load beyond the critical value. Analogous results are found for the average gap, tensile radius and solid-solid contact area. Such behavior suggests interface collapse, whereby beyond the critical point, the surfaces come into complete and near complete contact [33–36]. By introducing certain dimensionless parameters, the results can be generalized. Let an adhesion parameter Γ be defined according to

$$\Gamma \equiv \frac{\gamma\left(\cos\theta_1 + \cos\theta_2\right)V_o}{\pi\sqrt{2}A_n^{1/2}E'\sigma^3} \tag{69}$$

and let the dimensionless versions of external load, tensile force, and liquid volume be defined respectively as

$$P^* \equiv \frac{P}{\gamma V_o\left(\cos\theta_1 + \cos\theta_2\right)/\sigma^2} \tag{70}$$

$$F_t^* \equiv \frac{F_t}{\gamma V_o\left(\cos\theta_1 + \cos\theta_2\right)/\sigma^2} \tag{71}$$

$$V_o^* \equiv \frac{V_t}{A_n\sigma} \tag{72}$$

The results for dimensionless tensile force versus the adhesion parameter are depicted in Figure 13 at several values of dimensionless volume. This figure reveals that, for each dimensionless volume considered, there is a critical value of the adhesion parameter whereby the force curve becomes vertical, suggesting the onset of surface collapse.

http://dx.doi.org/10.5772/61572

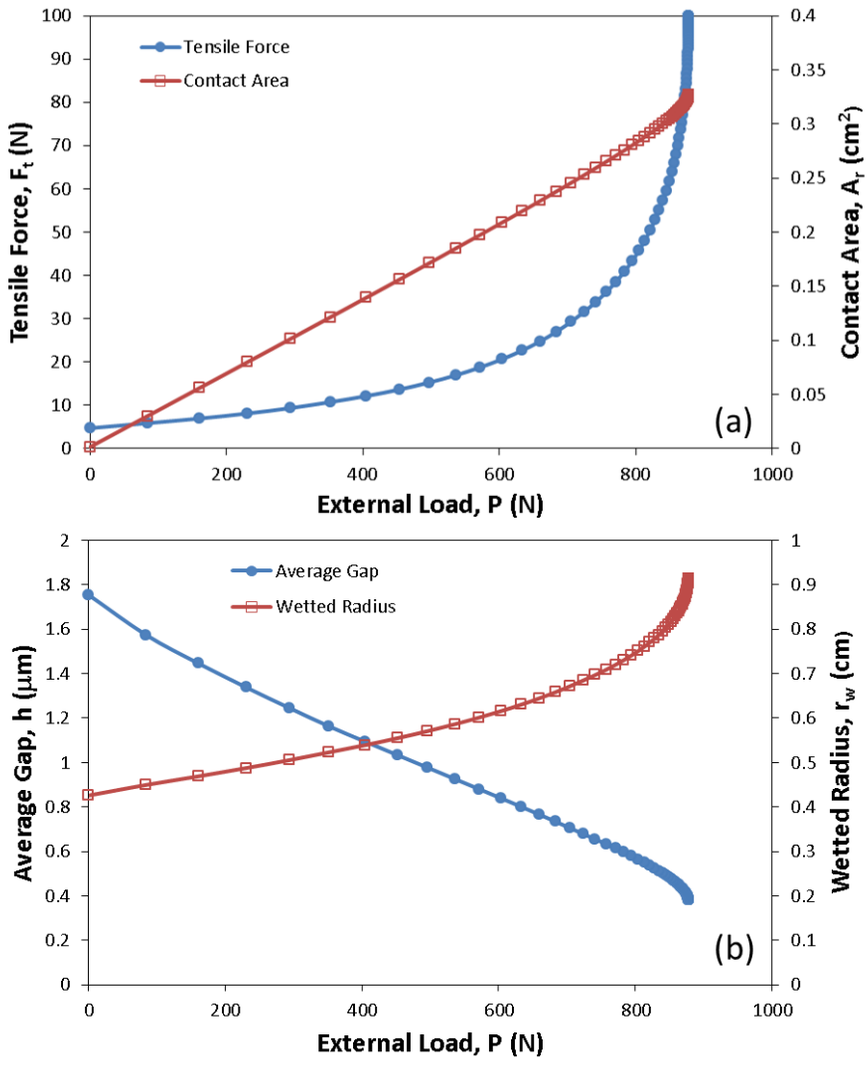

Figure 12. The effect of external load: (a) tensile force and contact area; (b) average gap and wetted radius.

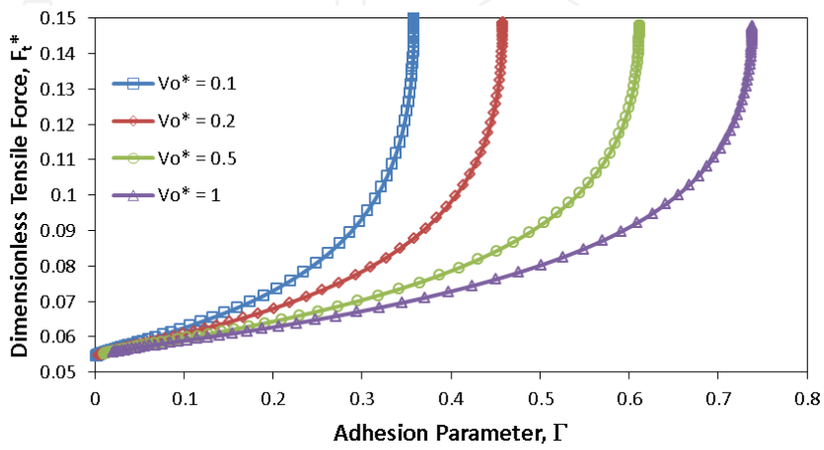

Figure 13. Dimensionless tensile force as a function of adhesion parameter for several dimensionless liquid volumes.

Acknowledgements

The author would like to thank the National Science Foundation (US) for support of this work and Amir Rostami, a graduate research assistant, for performing some calculations used herein.

Author details

Jeffrey L. Streator

Address all correspondence to: jeffrey.streator@me.gatech.edu

G.W. Woodruff School of Mechanical Engineering, Georgia Institute of Technology, Atlanta, GA, USA

References

[1] Bhushan B. Adhesion and stiction: Mechanisms, measurement techniques, and methods for reduction. Journal of Vacuum Science & Technology B. 2003;21(6):2262-2296.

[2] Van Spengen WM, Puers R, De Wolf I. A physical model to predict stiction in MEMS. Journal of Micromechanics and Microengineering. 2002;12(5):702.

[3] Van Spengen WM, Puers R, De Wolf I. On the physics of stiction and its impact on the reliability of microstructures. Journal of Adhesion Science and Technology. 2003;17(4):563-582.

[4] Komvopoulos K. Adhesion and friction forces in microelectromechanical systems: Mechanisms, measurement, surface modification techniques, and adhesion theory. Journal of Adhesion Science and Technology. 2003;17(4):477-517.

[5] Liu H, Bhushan B. Adhesion and friction studies of microelectromechanical systems/nanoelectromechanical systems materials using a novel microtriboapparatus. Journal of Vacuum Science & Technology A. 2003;21(4):1528-1538.

[6] Lee S-C, Polycarpou AA. Adhesion forces for sub-10 nm flying-height magnetic storage head disk interfaces. Journal of Tribology. 2004;126(2):334-341.

[7] Yang SH, Nosonovsky M, Zhang H, Chung K-H. Nanoscale water capillary bridges under deeply negative pressure. Chemical Physics Letters. 2008;451(1):88-92.

[8] Adamson AW, Gast AP. Physical chemistry of surfaces: JWiley and Sons. New York; 1967.

[9] Cai S, Bhushan B. Meniscus and viscous force during separation of hydrophilic and hydrophobic smooth/rough surfaces with symmetric and asymmetric contact angles. Philosophical Transactions of the Royal Society A. 2008;366:1627-1547. DOI: 10.1098/rsta.2007.2176.

[10] Hamrock BJ. Fundamentals of fluid film lubrication: McGraw-Hill; 1994.

[11] Munson BR, Okiishi TH, Huebsch WW, Rothmayer AP. Fundamentals of fluid mechanics, 7th ed. New York: Wiley; 2015.

[12] Sedgewick SA, Travena DH. Limiting negative pressure of water under dynamic stressing. Journal of Physics D. 1976; 9(14):1983-1990.

[13] Sun DC, Brewe DE. A high speed photography study of cavitation in a dynamically load journal bearing. Journal of Tribology. 1991;113(2):287-292.

[14] Braun MJ, Hannon WM. Cavitation formation and modeling for fluid film bearings: A review. Journal of Engineering Tribology. 2010;224(9):839-863.

[15] Roemer DB, Johansen P, Pedersen HC, Anderson TO. Fluid stiction modeling for quickly separating plates considering the liquid tensile strength. Journal of Fluids Engineering. 2015;137:061205:1-8

[16] Israelachvilli JN. Intermolecular and surface forces, 2nd ed. Academic Press, London; 1992.

[17] de Boer MP. Capillary adhesion between elastically hard rough surfaces. Experimental Mechanics. 2007;47:171-183. DOI: 10.1007/s11340-006-0631-z.

[18] [18]de Boer, MP, de Boer, PCT. Thermodynaics of capillary adhesion between rough surfaces. Journal of Colloid and Interface Science. 2007;311:171-185. DOI: 10.1007/s11340-006-0631-z.

[19] DelRio FW, Dunn ML, de Boer MP. Capillary adhesion model for contacting micromachined surfaces. Scripta Materialia. 2008;59:916-920. DOI: 10.1016/j-scriptamat.2008.02.037.

[20] Persson BNJ. Capillary adhesion between elastic solids with randomly rough surfaces. Journal of Physics of Condensed Matter. 2008;20:315007. DOI: 10.10088/0953-8984/20/31/314007.

[21] Peng YF, Guo YB, Hong YQ. An adhesion model for elastic-contacting fractal surfaces in presence of meniscus. Journal of Tribology. 2009;131:024504.

[22] Butt H-J, Barnes WJP, del Campo A, Kappl M, Schonfeld F. Capillary forces between soft elastic spheres. Soft Matter. 2010;6:5930-5936.

[23] Men Y, Zhang Z, Wenchuan W. Capillary liquid bridges in atomic force microscopy: Formation, rupture and hysteresis. Journal of Chemical Physics. 2009;131:184702.

[24] Rabinovich YI, Esayanur MS, Moudgil BM. Capillary forces between two spheres with a fixed volume liquid bridge: Theory and experiment. Langmuir. 2005;21:10992-10997.

[25] Streator JL. Analytical instability model for the separation of a sphere from a flat in the presence of a liquid. Proceedings of the ASME/STLE International Joint Tribology Conference, IJTC 2004. 2004; Part B: 1197-1204.

[26] Chan DYC, Horn RG. The drainage of thin liquid films between solid surfaces. Journal of Chemical Physics.1985;83(10);4311-5324.

[27] Matthewson M. Adhesion of spheres by thin liquid films. Philosophical Magazine A. 1988;57(2):207-216.

[28] Zheng J, Streator J. A liquid bridge between two elastic half-spaces: A theoretical study of interface instability. Tribology Letters. 2004;16(1-2):1-9.

[29] Johnson KL, Johnson KL. Contact mechanics: Cambridge University Press; 1987.

[30] Zheng J, Streator JL. A micro-scale liquid bridge between two elastic spheres: Deformation and stability. Tribology Letters. 2003;15(4):453-464.

[31] Zheng J, Streator J. A generalized formulation for the contact between elastic spheres: Applicability to both wet and dry conditions. Journal of Tribology. 2007;129:274.

[32] Johnson KL, Kendall, K, Roberts, AD. Surface energy and the contact of elastic solids. Proceedings of the Royal Society (London), Series A. 1971;324(1558):301-313.

[33] Streator JL. A model of liquid-mediated adhesion with a 2D rough surface. Tribology Interntional. 2009;42:1439-1447.

[34] Streator JL, Jackson RL. A model for the liquid-mediated collapse of 2-D rough surfaces. Wear. 2009;267(9):1436-1445.

[35] Rostami A, Streator JL. Study of Liquid-mediated adhesion betweeen 3D rough surfaces: A spectral approach. Tribology International. 2015;58(2):1-13.

[36] Rostami A, Streator JL. A deterministic approach to studying liquid-mediated adhesion between rough surfaces. Tribology Letters. 2015;84:36-47. DOI: 10.1007/s11249-015-0497-2.

[37] Wang L, Regnier S. A more general capillary adhesion model including shape index: Single-asperity and multi-asperity cases. Tribology Transacations. 2015;58:106-112. DOI: 10.1080/10402004.2014.951751.

[38] Jackson RL, Streator JL. A multi-scale model for contact between rough surfaces. Wear. 2006;261(11):1337-1347.